Modeling of Dispersive Transport in the Context of Negative Bias Temperature Instability

Tibor Grasser* , Wolfgang Gös* , and Ben Kaczer°

* Christian Doppler Laboratory for TCAD at the Institute for Microelectronics, Gußhausstraße 27–29, A-1040 Wien, Austria
° IMEC, Kapeldreef 75, B-3001 Leuven, Belgium

***Abstract*— Negative bias temperature instability (NBTI) is one of the most serious reliability concerns for highly scaled pMOSFETs. It is most commonly interpreted by some form of reaction-diffusion (RD) model, which assumes that some hydrogen species is released from previously passivated interface defects, which then diffuses into the oxide. It has been argued, however, that hydrogen motion in the oxide is trap-controlled, resulting in dispersive transport behavior. This defect-controlled transport modifies the characteristic exponent in the power-law that describes the threshold-voltage shift. However, previously published models are contradictory and both an increase and a decrease in the power-law exponent have been reported. We clarify this discrepancy by identifying the boundary condition which couples the transport equations to the electro-chemical reaction at the interface as the crucial component of the physically-based description.**

I. Introduction

Amongst the various reliability issues in modern CMOS technology, negative bias temperature instability (NBTI) has been identified as one of the most serious concerns for highly scaled pMOSFETs [1–4]. Recently, a lot of effort has been put into refining the classic reaction-diffusion theory [2, 5, 6] originally proposed by Jeppson and Svensson nearly thirty years ago [7, 8]. The RD model assumes that Si–H bonds at the interface are broken at higher temperatures and electric fields, causing the released hydrogen species to diffuse into the oxide. Analytic solutions of the RD model can been shown to follow a power-law [2]

$$\Delta V_{\rm th}(t) \propto \Delta N_{\rm it}(t) = A(T, E_{\rm ox})\, t^n \ , \qquad (1)$$

where the change in the threshold voltage is often assumed to be proportional to the change in the silicon dangling bond density $N_{\rm it} = [{\rm Si}^\bullet]$ at the interface. As diffusing species H_2 is often assumed because in the RD framework it results in a characteristic time exponent of $1/6$ for the threshold shift, consistent with recent no-delay measurements [9], while H^0 and H^+ result in $n = 1/4$ and $n = 1/2$, respectively [5].

During the last couple of years a variety of alternative explanations for NBTI have been put forward [3, 10–13]. In particular it has been argued that transport of the hydrogen species inside the oxide is dispersive [2, 10–12], consistent with hydrogen diffusion measurements and available models for irradiation damage. Interestingly, in these models the slope depends on a temperature-dependent dispersion parameter. Also, it is possible to incorporate technology-dependent behavior into the model by adjusting the dispersion parameter. In addition, these models brought H^+ back into the game, which had originally been dismissed due to the $1/2$ slope resulting from the RD model.

One feature common to trap-controlled dispersive NBTI models is that they predict that dispersive diffusion *reduces* the slope compared to their conventional counterparts [10–12]. However, in contrast to that it was observed that inclusion of traps into a standard RD model *increases* the slope [5]. In addition, our own simulations showed [14] that a straight-forward application of the multiple-trapping transport model [15, 16], which is the basis for many dispersive transport models [17], *increases* the slope, also in contradiction to published reaction-dispersive-diffusion models [2, 10–12]. A detailed analysis reveals that the boundary condition at the Si/SiO_2 interface is the main reason for this discrepancy. It is shown that the choice of the boundary condition is essential for the overall behavior of the dispersive system.

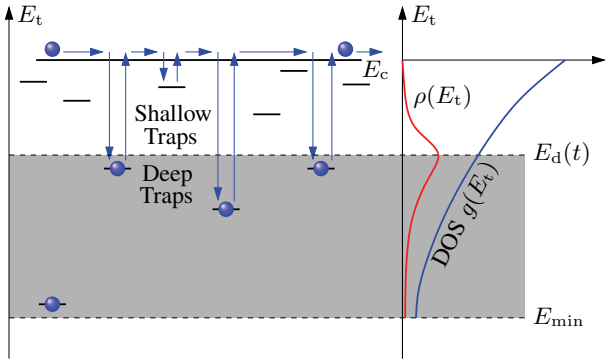

Fig. 1. Schematic illustration of dispersive transport. Particles in the conduction band fall into the traps and are re-emitted into the conduction band. Re-emission is more likely for shallow traps. The time-dependent demarcation energy separates shallow from deep traps. With time, the demarcation energy becomes more negative, until the bottom of the trap distribution is reached and equilibrium is obtained. As a result, the motion of the particle packet slows down with time. Note how the individual trap levels, which microscopically correspond to the different bonding energies of hydrogen in an amorphous material, are approximated by a macroscopic density-of-states.

II. Dispersive Transport

In contrast to drift-diffusion transport, dispersive transport is trap-controlled. This implies that most particles are trapped, that is, bonded. Depending on the bonding energy (the distance to the 'conduction band') hydrogen can be easily released from shallow traps but have large release times from deep traps. This is schematically illustrated in Fig. 1.

Reaction-dispersive-diffusion models proposed so far have relied on simplified transport models developed either for the time evolution of an initial hydrogen profile after an irradiation pulse [11, 12] or on a phenomenological time-dependent diffusivity as observed in hydrogen diffusion and annealing experiments [18]. The applicability of these simplified equations to the problem at hand has not been rigorously assessed and, as we will show in the following, contains some pitfalls: First, during NBTI stress, one has to deal with a continuous influx of particles which has to be properly accounted for in the boundary condition of the model equations. Care has to be taken to inject the particles into the mobile state only, an issue often not obvious in simplified equation sets. Second, the reverse rate of the depassivating reaction depends on the concentration of available hydrogen at the interface. Here, one might have to consider

1-4244-0297-2/06/$20.00 ©2006 IEEE

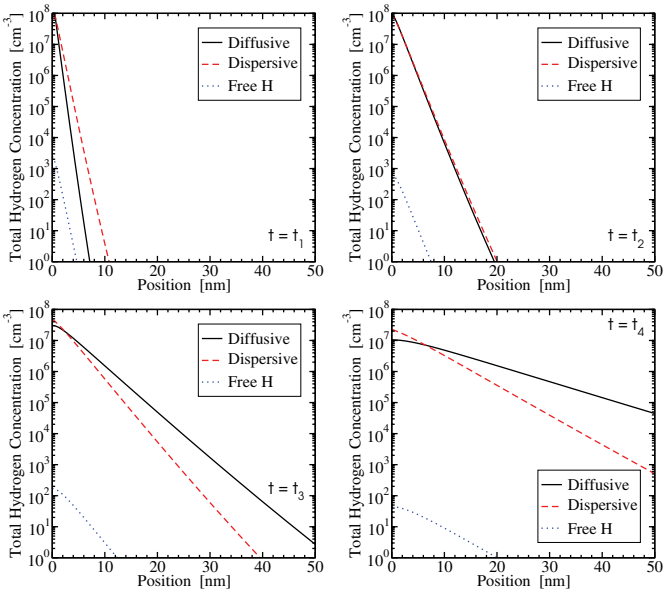

Fig. 2. Comparison of the hydrogen profiles at different time points for classic diffusion versus dispersive diffusion. Shown is the one-sided broadening of an initial particle sheet $H_0(x) = H_{\text{init}}\delta(x)$. For the classic case, the diffusivity was set to $D = D_c \times 10^{-4}$ in order to accommodate both profiles on the same plot. Note that the free hydrogen concentration in the conduction band (dotted line) is much smaller than the concentration of the trapped hydrogen (dashed line) and that the profile is steeper, that is, remains closer to the initial position.

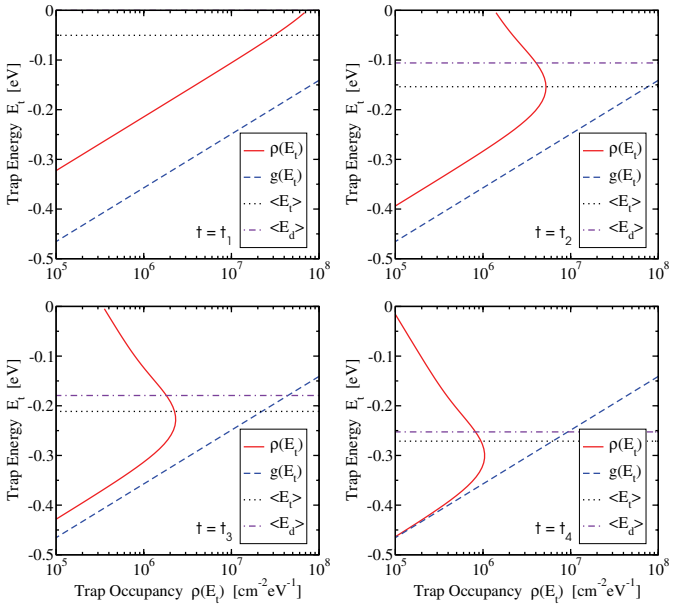

Fig. 3. Evolution of the trapped hydrogen profile with time for the diffusion process given in Fig. 2. Shown is the density $\rho(E_t)$ right at the interface ($x = 0$). At early time points ($t = t_1$) the profile closely resembles the exponential density-of-states. Particles residing on shallow traps closer to $E_c = 0$ are easily emitted in a process that consequently favors the occupancy of the deeper trap levels. This results in the characteristics humps that can be observed for $t > t_1$. Note that the average energy of the trapped hydrogen, $\langle E_t \rangle$, roughly corresponds to the demarcation energy E_d.

that in the dispersive case most particles are trapped, that is, bonded, rather than in the 'conduction state'. As will be shown, this issue is of fundamental importance to the model as it results in completely different time slopes.

A. *Multiple-Trapping Model*

Dispersive transport is often described using the continuous time random walk (CTRW) theory [19] or multiple-trapping (MT) models [15–17]. Both models exhibit similar features [20–22] and will be considered equivalent in the following [21]. The MT model equations consist of a continuity equation and the corresponding flux relation

$$\frac{\partial H_c}{\partial t} = -\nabla \cdot \mathbf{f}_c - \int \frac{\partial \rho}{\partial t}\,\mathrm{d}E_t \;, \tag{2}$$

$$\mathbf{f}_c \quad = -D_c\Big(\nabla H_c - \frac{Z}{V_T} H_c \mathbf{E}\Big) \;. \tag{3}$$

Here, H_c is the hydrogen concentration in the conduction state, D_c the diffusivity in the conduction state, Z the charge state of the particle, V_T the thermal voltage, $\mathbf{E}$ the electric field, while $\rho(E_t)$ and $g(E_t)$ are the trapped hydrogen density ($\mathrm{cm}^{-3}\mathrm{eV}^{-1}$) and density-of-states ($\mathrm{cm}^{-3}\mathrm{eV}^{-1}$) at the trap level E_t. The trap occupancy is governed by balance equations which have to be solved for each trap level

$$\frac{\partial \rho(E_t)}{\partial t} = \underbrace{\frac{\nu_0}{N_c}(g(E_t) - \rho(E_t))H_c}_{\text{capture}} \tag{4}$$

$$\underbrace{- \nu_0 \exp\Big(-\frac{E_c - E_t}{k_B T_L}\Big)\rho(E_t)}_{\text{release}} \;, \tag{5}$$

with ν_0 being the attempt frequency, N_c the effective density-of-states in the conduction band, T_L the lattice temperature, and E_c the conduction band edge (assumed to be zero in the following). In our context it is worthwhile to recall that the total hydrogen concentration consists of hydrogen in the conduction states $H_c(x,t)$ and trapped hydrogen as

$$H(\mathbf{x},t) = H_c(\mathbf{x},t) + \int \rho(\mathbf{x},E_t,t)\,\mathrm{d}E_t \tag{6}$$

An exponential density-of-states is commonly assumed [12, 17]

$$g(E_t) = \frac{N_t}{E_0}\exp\Big(-\frac{E_c - E_t}{E_0}\Big) \;, \tag{7}$$

which, in this particular context, results in a power-law for $N_{it}(t)$.

Qualitatively, the system responds as follows if brought out of equilibrium:

- At the initial stage, the capture rate (first term) in (5) dominates. Since ρ will still be small, the distribution will closely resemble the density-of-states (cf. Fig. 3).
- Then, since the release term depends exponentially on the distance of the trap level from the conduction band, particles on shallower traps (traps 'closer' to E_c) are more likely to be released than deeper traps. As a consequence, the shallower trap levels become depleted while particles accumulate in the 'deep' traps. This is the non-equilibrium regime.
- The transition between 'shallow' and 'deep' traps is described by the demarcation energy

$$E_d(t) = E_c - k_B T_L \log \nu_0 t \;, \tag{8}$$

which becomes more negative with time.
- As soon as the demarcation energy reaches the 'bottom' of the density-of-states, equilibrium is obtained, and the system behaves similarly to a non-dispersive one, although a different 'effective' diffusivity and temperature dependence are observed. Note, that from a mathematical point of view, this never happens for an ideal exponential density-of-states such as (7) [17].

The evolution of an initial particle sheet with time is shown in Fig. 2 while the trapped hydrogen profile $\rho(E_\mathrm{t},t)$ is depicted in Fig. 3.

B. Extremely Non-Equilibrium Approximation

As the MT equations are rather complex and can in general only be solved numerically, simplified equations have been derived [17], valid in the extremely non-equilibrium case (EN-MT model). The approximation relies on the existence of the demarcation energy separating shallow from deep traps. The shallow traps are assumed to be in equilibrium with the conducting states while the deep traps create the dispersion due to the time dependent demarcation energy. Ignoring the initial early times and the possible final equilibration, one can show that the broadening of an initial particle distribution $H_0(\mathbf{x})$ is given through

$$\frac{H(\mathbf{x},t)-H_0(\mathbf{x})}{\tau(t)} = -\nabla\cdot\mathbf{F}(\mathbf{x},t)\ . \tag{9}$$

Here the flux is given through an 'effective' flux of the total concentration of the species H

$$\mathbf{F} = -D_\mathrm{c}\Big(\nabla H - \frac{Z}{V_\mathrm{T}}H\mathbf{E}\Big)\ , \tag{10}$$

rather than the concentration in the conduction states H_c. Note also, that there is no time derivative in (9) and the dynamics of the system can be incorporated into $\tau(t)$, which directly depends on the hydrogen trap density-of-states

$$\tau(t) = \Big[\frac{\nu_0}{N_\mathrm{c}}\int_{E_\mathrm{d}(t)}^{\infty} g(E_\mathrm{t})\ \mathrm{d}E_\mathrm{t}\Big]^{-1}\ . \tag{11}$$

Of particular interest in our context is the concentration of the 'free' hydrogen H_c, which is directly linked to the total hydrogen concentration H and can be approximated in the non-equilibrium regime as [17]

$$H_\mathrm{c}(\mathbf{x},t) = \frac{\partial\,\tau(t)H(\mathbf{x},t)}{\partial t}\ . \tag{12}$$

It is important to recall in our context that (9) was derived to describe the broadening of an initial particle distribution H_0, such as in Fig. 2. However, things are different during NBT stress where we have to deal with a continuous injection of particles into the oxide during the stress phase. A generalization of the original derivation reveals that (9) is still valid, provided the boundary condition is modified according to

$$\mathbf{F}_\mathrm{c}(t) = \int_0^t \mathbf{f}_\mathrm{c}(t')\ \mathrm{d}t'\ , \tag{13}$$

with $\mathbf{f}_\mathrm{c}(t)$ being the particle influx at time t. Note that (13) is only valid in the extremely non-equilibrium case which will be assumed to be prevalent in the following. The boundary condition (13) will be used for the numerical evaluation of (9).

III. Dispersive Transport and NBTI

In order to obtain an NBTI model, the transport equation has to be coupled to the electro-chemical reaction assumed to take place at the interface. As in the RD model [8, 23, 24], the kinetic equation describing the interface reaction is assumed to be of the form

$$\frac{\partial N_\mathrm{it}}{\partial t} = k_\mathrm{f}(N_0-N_\mathrm{it}) - k_\mathrm{r}N_\mathrm{it}H_\mathrm{it}^{1/a}\ . \tag{14}$$

where N_it is the surface state concentration, N_0 the initial concentration of passivated interface defects, H_it the interfacial hydrogen concentration, k_f and k_r the field and temperature dependent rate coefficients, while a is the kinetic exponent (1 for H^0 and H^+, and 2 for H_2) [24].

As a boundary condition to the transport equations one has

$$\mathbf{f}_\mathrm{c}(t)\cdot\mathbf{n} = \frac{1}{a}\frac{\partial N_\mathrm{it}}{\partial t}\ , \tag{15}$$

with $\mathbf{n}$ being the normal vector at the interface. For the non-equilibrium approximation we obtain through (13)

$$\mathbf{F}_\mathrm{c}(t)\cdot\mathbf{n} = \frac{N_\mathrm{it}(t)-N_\mathrm{it}(0)}{a}\ . \tag{16}$$

Classic and dispersive NBTI models assume the interface reaction to be in quasi-equilibrium ($\partial N_\mathrm{it}/\partial t\approx 0$) [2, 10, 12]. From (14) one obtains by neglecting saturation effects ($N_\mathrm{it}\ll N_0$)

$$\frac{k_\mathrm{f}N_0}{k_\mathrm{r}} = N_\mathrm{it}H_\mathrm{it}^{1/a}\ . \tag{17}$$

A. Total Hydrogen Boundary Condition

The fundamental question in the context of dispersive transport is how to determine the interfacial hydrogen concentration H_it. In [12] it was assumed that the NBTI reverse reaction is driven by the *total* hydrogen concentration at the interface, that is $H_\mathrm{it}(t)=H(0,t)$.

Equation (9) is straight forward to solve and assuming the interface at $x=0$, the total hydrogen concentration in the positive half-space is given as

$$H(x,t) = H(0,t)\exp\Big(-\frac{x}{\lambda(t)}\Big)\ , \tag{18}$$

with $\lambda(t)=\sqrt{D_\mathrm{c}\tau(t)}$ for neutral particles and $\lambda(t)=\mu_\mathrm{c}E_\mathrm{ox}\tau(t)$ for protons [12], with $\mu_\mathrm{c}=\mathrm{q}D_\mathrm{c}/\mathrm{k_B}T_\mathrm{L}$.

Integrating (9) over the half-space $x>0$ we obtain with (16) and (18) together with $N_\mathrm{it}(0)=0$ and $H_0(\mathbf{x},0)=0$

$$N_\mathrm{it}(t) = a\lambda(t)H(0,t)\ . \tag{19}$$

Assuming $H_\mathrm{it}(t)=H(0,t)$ and plugging (19) into (17) we obtain for neutral particles ($Z=0$)

$$N_\mathrm{it}(t) = A\Big(\frac{N_\mathrm{c}}{N_\mathrm{t}}\Big)^{1/(2+2a)}(\nu_0 t)^{\alpha/(2+2a)}\ , \tag{20}$$

with the dispersion parameter

$$\alpha = \mathrm{k_B}T_\mathrm{L}/E_0\ . \tag{21}$$

The prefactor A is given through

$$A = (k_\mathrm{f}N_0/k_\mathrm{r})^{a/(1+a)}(a^2D/\nu_0)^{1/(2+2a)}\ . \tag{22}$$

For atomic hydrogen ($a=1$) the slope is given through $n=\alpha/4$ while molecular hydrogen ($a=2$) gives $n=\alpha/6$. Since α equals 1 in the diffusive limit and 0 in the extremely dispersive case, (20) implies that for dispersive transport a slope *smaller* than the RD slopes of $1/4$ and $1/6$ can be obtained. Also, for increasing trap density N_t, the total amount of degradation *decreases*. With $Z=1$ and the approximate relation for $\lambda(t)$ we obtain $n=\alpha/2$ for H^+. Note that the numerical solution for H^+ contains a transitional region with $n=\alpha/4$, where the diffusive component still dominates.

Qualitatively, this means that dispersive transport results in most particles being trapped close to the interface, resulting in a steeper profile compared to classic diffusion. However, as *all* hydrogen is available for the reverse rate in (14), the net interface state generation is suppressed, resulting in a smaller slope.

Since the dispersion parameter α depends linearly on the temperature, a linear temperature dependence of the slope is obtained as [12]

$$n_1 = \frac{\alpha}{2+2a} = \frac{\mathrm{k_B}T_\mathrm{L}}{2E_0(1+a)}\ . \tag{23}$$

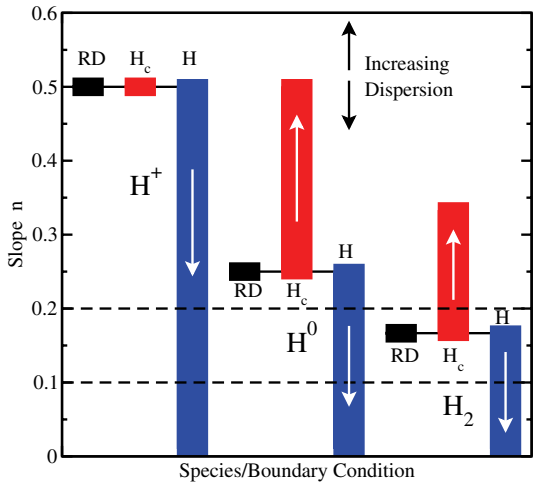

Fig. 4. The possible slopes for the two boundary conditions and the three investigated species H^+, H^0, and H_2. For the boundary condition $H_{it} = H_c$ a slope *larger* than the RD equivalent is obtained while the boundary condition $H_{it} = H$ results in the opposite behavior. Also (roughly) indicated is the range of slopes observed during on-the-fly measurements, $n \approx 0.1 - 0.2$.

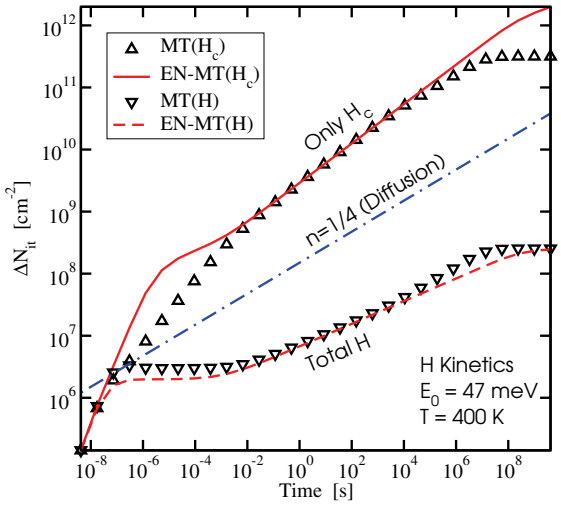

Fig. 5. Interface state density as a function of the boundary condition calculated numerically by solving the MT and EN-MT equations. Saturation occurs as soon as the hydrogen diffusion front reaches the other side of the oxide layer, where a perfectly reflecting boundary condition was used in the numerical solutions. The approximations underlying the EN-MT equations seem to be well justified.

This is consistent with experimental results [3, 12]. It has to be kept in mind, however, that these data were obtained using delayed measurements and also temperature-independent slopes for delay-free measurements have been reported [9].

B. Conduction State Hydrogen Boundary Condition

In contrast, if we now assume that only the free hydrogen can participate in the reverse rate, that is $H_{it} = H_c(0)$, which is the 'natural' boundary condition for the MT model [25], one obtains

$$\frac{k_f N_0}{k_r} = N_{it}(t)\left(N_{it}(t)\frac{\partial\frac{\tau(t)}{a\lambda(t)}}{\partial t} + \frac{\tau(t)}{a\lambda(t)}\frac{\partial N_{it}(t)}{\partial t}\right)^{1/a} , \qquad (24)$$

which for neutral particles ($Z = 0$) has the solution

$$N_{it}(t) = A\left(\frac{N_t}{N_c}\right)^{1/(2+2a)}\left(\frac{1+a}{1+a\alpha/2}\right)^{1/(1+a)}(\nu_0 t)^{(1-\alpha/2)/(1+a)} . \qquad (25)$$

For atomic hydrogen, the slope $n = 1/2 - \alpha/4$ is obtained while H_2 results in $n = 1/3 - \alpha/6$. Hence, for increased dispersion the slopes become now *larger* than their RD equivalents. Furthermore, when the trap density is increased, the degradation *increases*. In contrast, H^+ results in $n = 1/2$, which is equal to the classic result and independent of the dispersion parameter!

Again, qualitatively, the newly released hydrogen quickly falls into the traps (becomes bonded again), but since for times larger than $1/\nu_0$ most hydrogen resides in deep traps and is therefore not as easily available for the reverse rate in (14). This suppresses the reverse reaction and consequently enhances the net interface state generation and results in a larger slope.

In contrast to the previous boundary condition, now the slope decreases with increasing temperature through

$$n_2 = \frac{1-\alpha/2}{1+a} = \frac{2E_0 - k_B T_L}{2E_0(1+a)} = \frac{1}{1+a} - n_1 . \qquad (26)$$

This is in contradiction to currently available observations [3, 9, 12].

The possible slopes for the various combinations of boundary condition and species are compared in Fig. 4.

C. Alternative Models

Instead of the MT model, an approximate solution for the CTRW models was employed by Houssa *et al.* [11]. Again, this approximate solution was derived for the broadening of an initial concentration [26], and since CTRW and MT theory are in many ways compatible [20, 21], we assume our results of the MT model to also apply to models derived from the CTRW theory.

Instead of MT or CTRW solutions, models based on a phenomenological time-dependent diffusivity

$$D(t) = D_0(\nu t)^{-(1-\alpha)} , \qquad (27)$$

have been used [2, 10]. Here, D_0 is the microscopic diffusivity, ν an attempt frequency different to ν_0, and α the dispersion parameter [27]. As in the MT model for an exponentially decreasing trap density, α is given as $\alpha = k_B T_L/E_0$, where E_0 is the characteristic energy. Since (27) is derived by matching SIMS measurements, this model does not allow one to differentiate between free and trapped hydrogen, which has a significant influence on the NBTI boundary condition as shown below.

IV. Model Comparison

A numerical solution of the MT model was used as a reference model. For the numerical solution the trap density-of-states was discretized using 20 energy points while the energy range was limited to the interval $E_{max} = 0\,eV$ and $E_{min} = -20E_0$. This implies that as soon as the demarcation energy E_d reaches E_{min}, a transition from the dispersive to the classic diffusive regime is observed. Note that this transition is not available in the approximate solutions described above. As the exact value of E_{min} is essentially unknown, it was set to a value small enough so as not to influence the numerical solution. Furthermore, the numerical solution considers the trap occupancy in the capture rate of (5), which is also not contained in the approximate solutions. This trap occupancy results in a transition from dispersive to conventional diffusion as soon as all traps are filled. Such a transition might be relevant and can also be experimentally observed for hydrogen concentrations larger than

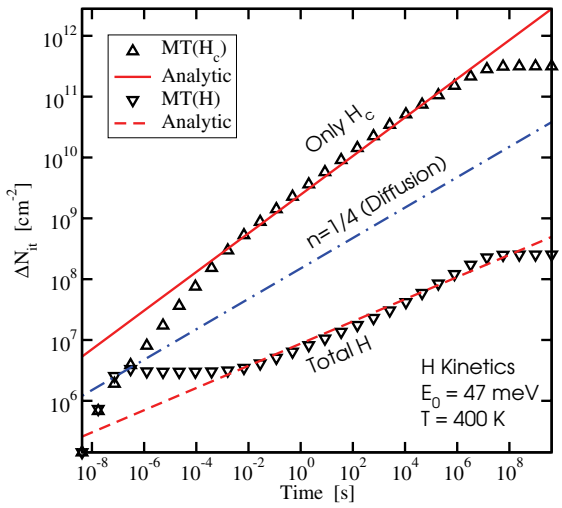

Fig. 6. Interface state density as a function of the boundary condition calculated numerically by solving the MT equations in comparison to the analytic expressions (20) and (25). Again, good agreement is obtained for both boundary conditions.

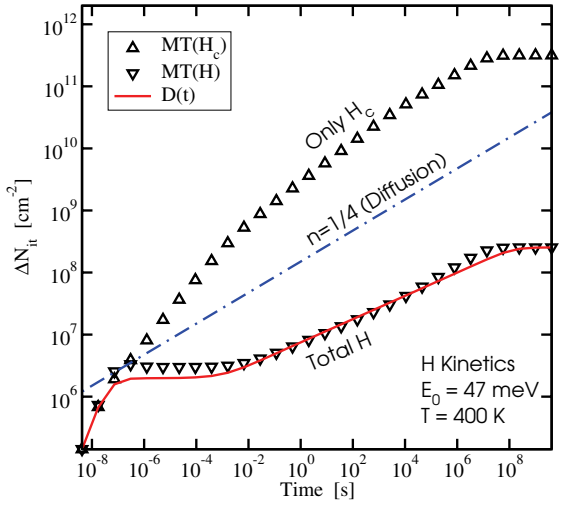

Fig. 7. Comparison of the calculated interface state density obtained from numerically solving the diffusion equation with a time-dependent diffusivity. Good agreement for the case $H_{\mathrm{it}} = H$ is obtained.

the trap density [18]. However, this effect is neglected here for the sake of a straight-forward comparison.

In a first step the applicability of the Arkhipov model to NBTI is investigated. For this the numerical solutions of the MT and the EN-MT equations are compared in Fig. 5 where good agreement is observed for each boundary condition, thereby justifying the underlying approximations. Next, the analytical expressions (20) and (25) are compared to the numerical solutions of the MT equations in Fig. 6. Again, good agreement is obtained in the quasi-equilibrium (diffusion-limited) regime. Of course, no reaction-limited regime and saturation can be observed. Finally, the numerical result obtained from a standard reaction-diffusion model with a time-dependent diffusivity [10] is shown in Fig. 7. Interestingly, the simple phenomenological model captures the case where the total hydrogen participates in the reverse rate ($H_{\mathrm{it}} = H$) very well. However, the applicability of this phenomenological model to the relaxation case needs to be investigated.

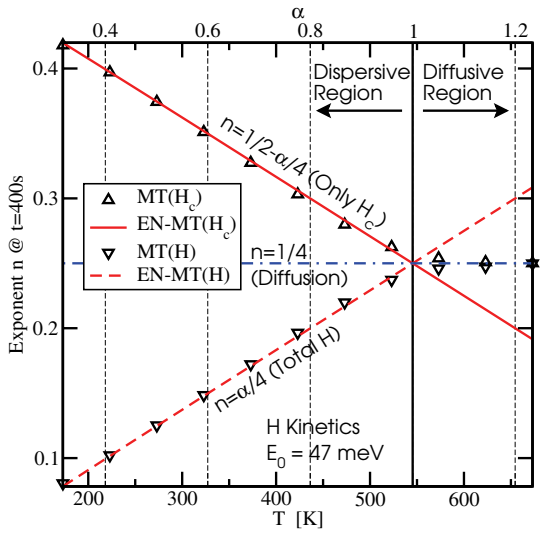

Fig. 8. Temperature dependence of the slope for the two boundary conditions. As expected from the derivation, the EN-MT model breaks down for the case when the trap density-of-states becomes to narrow for dispersive transport to occur ($\alpha > 1$), while the MT model correctly reproduces the diffusive limit with $n = 1/4$.

The temperature dependence of the slopes predicted by the analytic expressions (20) and (25) are compared to the full numerical results in Fig. 8. Note that the system is only dispersive as long as the characteristic energy E_0 in the density-of-states (7) is larger than the thermal energy $\mathrm{k_B}T_{\mathrm{L}}$ [17]. In terms of the dispersion parameter α this means $\alpha < 1$. This also implies that for increasing temperatures a transition to classic transport is observed as soon as E_0 becomes smaller than the thermal energy $\mathrm{k_B}T_{\mathrm{L}}$, that is, $\alpha > 1$. Since the dispersive models are derived under the assumption $\alpha < 1$, the cannot reproduce the full numerical results in that regime, but give excellent agreement for $\alpha < 1$.

The good agreement between the numerical and analytic result indicates that the simplifying assumptions in the derivation of (20) and (25) are well justified, which are worth summarizing:

- The dynamics are solely determined by carrier trapping and detrapping.
- The continuous injection of particles is too slow ($\partial N_{\mathrm{it}}/\partial t \approx 0$) to seriously disrupt the extremely non-equilibrium assumption with a single demarcation energy.
- The amount of hydrogen that is allowed to participate in the NBTI reverse reaction determines the overall dynamics, that is, this boundary condition determines whether an increase or a decrease in the slope is observed.
- The interface reaction is in quasi-equilibrium.

V. Conclusions

Clearly, the question of what boundary condition for the reverse rate in the NBTI model captures the microscopic physics best is of utmost importance. For the present analysis we have to keep in mind that the macroscopic density-of-states is derived for a amorphous bulk material and is unlikely to be valid next to an interface. In that context, the physical mechanisms justifying the 'conduction band' concept in conjunction with hydrogen hopping next to the interface need to be evaluated and justified.

Under the assumption that this concept remains nevertheless valid, we have investigated two different boundary conditions: Provided

that only hydrogen in the multiple-trapping conduction band can passivate dangling bonds, only H_2 in a reaction-dispersive-diffusion model gives slopes compatible with measurements and would allow to explain (temperature-dependent) delay-free slopes larger than $1/6$. In contrast, if all the trapped hydrogen can be involved, the previously published NBTI models [2, 10–12] remain valid, reproducing (temperature-dependent) measured slopes also with H^0 and H^+ kinetics.

REFERENCES

[1] D.K. Schroder and J.A. Babcock, "Negative Bias Temperature Instability: Road to Cross in Deep Submicron Silicon Semiconductor Manufacturing," *J.Appl.Phys.*, vol. 94, no. 1, pp. 1–18, 2003.

[2] M.A. Alam and S. Mahapatra, "A Comprehensive Model of PMOS NBTI Degradation," *Microelectr.Reliab.*, vol. 45, no. 1, pp. 71–81, 2005.

[3] V. Huard, M. Denais, and C. Parthasarathy, "NBTI Degradation: From Physical Mechanisms to Modelling," *Microelectr.Reliab.*, vol. 46, no. 1, pp. 1–23, 2006.

[4] J.H. Stathis and S. Zafar, "The Negative Bias Temperature Instability in MOS Devices: A Review," *Microelectr.Reliab.*, vol. 46, no. 2-4, pp. 270–286, 2006.

[5] S. Chakravarthi, A.T. Krishnan, V. Reddy, C.F. Machala, and S. Krishnan, "A Comprehensive Framework for Predictive Modeling of Negative Bias Temperature Instability," in *Proc. IRPS*, 2004, pp. 273–282.

[6] A.T. Krishnan, C. Chancellor, S. Chakravarthi, P.E. Nicollian, V. Reddy, A. Varghese, R.B. Khamankar, and S. Krishnan, "Material Dependence of Hydrogen Diffusion: Implications for NBTI Degradation," in *Proc. IEDM*, 2005, pp. 688–691.

[7] K.O. Jeppson and C.M. Svensson, "Negative Bias Stress of MOS Devices at High Electric Fields and Degradation of MNOS Devices," *J.Appl.Phys.*, vol. 48, no. 5, pp. 2004–2014, 1977.

[8] S. Ogawa and N. Shiono, "Generalized Diffusion-Reaction Model for the Low-Field Charge Build Up Instability at the Si/SiO2 Interface," *Phys.Rev.B*, vol. 51, no. 7, pp. 4218–4230, 1995.

[9] D. Varghese, D. Saha, S. Mahapatra, K. Ahmed, F. Nouri, and M. Alam, "On the Dispersive versus Arrhenius Temperature Activation of NBTI Time Evolution in Plasma Nitrided Gate Oxides: Measurements, Theory, and Implications," in *Proc. IEDM*, Dec. 2005, pp. 1–4.

[10] S. Zafar, "Statistical Mechanics Based Model for Negative Bias Temperature Instability Induced Degradation," *J.Appl.Phys.*, vol. 97, no. 10, pp. 1–9, 2005.

[11] M. Houssa, M. Aoulaiche, S. De Gendt, G. Groeseneken, M.M. Heyns, and A. Stesmans, "Reaction-Dispersive Proton Transport Model for Negative Bias Temperature Instabilities," *Appl.Phys.Lett.*, vol. 86, no. 9, pp. 1–3, 2005.

[12] B. Kaczer, V. Arkhipov, R. Degraeve, N. Collaert, G. Groeseneken, and M. Goodwin, "Disorder-Controlled-Kinetics Model for Negative Bias Temperature Instability and its Experimental Verifi cation," in *Proc. IRPS*, 2005, pp. 381–387.

[13] L. Tsetseris, X.J. Zhou, D.M. Fleetwood, R.D. Schrimpf, and S.T. Pantelides, "Physical Mechanisms of Negative-Bias Temperature Instability," *Appl.Phys.Lett.*, vol. 86, no. 14, pp. 1–3, 2005.

[14] T. Grasser, R. Entner, O. Triebl, H. Enichlmair, and R. Minixhofer, "TCAD Modeling of Negative Bias Temperature Instability," in *Proc. SISPAD*, Monterey, USA, Sept. 2006, pp. 330–333.

[15] J. Noolandi, "Multiple-Trapping Model of Anomalous Transit-Time Dispersion in α-Se," *Phys.Rev.B*, vol. 16, no. 10, pp. 4466–4473, 1977.

[16] J. Orenstein, M.A. Kastner, and V. Vaninov, "Transient Photoconductivity and Photo-Induced Optical Absorption in Amorphous Semiconductors.," *Philos.Mag.B*, vol. 46, no. 1, pp. 23–62, 1982.

[17] V.I. Arkhipov and A.I. Rudenko, "Drift and Diffusion in Materials with Traps," *Philos.Mag.B*, vol. 45, no. 2, pp. 189–207, 1982.

[18] N.H. Nickel, W.B. Jackson, and J. Walker, "Hydrogen Migration in Polycrystalline Silicon," *Phys.Rev.B*, vol. 53, no. 12, pp. 7750–7761, 1996.

[19] H. Scher and E.W. Montroll, "Anomalous Transit-Time Dispersion in Amorphous Solids," *Phys.Rev.B*, vol. 12, no. 6, pp. 2455–2477, 1975.

[20] V.I. Arkhipov, "Trap-Controlled and Hopping Modes of Transport and Recombination: Similarities and Differences," in *Proc. ISEIM*, 1995, pp. 271–274.

[21] J. Noolandi, "Equivalence of Multiple-Trapping Model and Time-Dependent Random Walk," *Phys.Rev.B*, vol. 16, no. 10, pp. 4474–4479, 1977.

[22] F.W. Schmidlin, "Theory of Trap-Controlled Photoconduction," *Phys.Rev.B*, vol. 16, no. 6, pp. 2362–2385, 1977.

[23] S. Ogawa, M. Shimaya, and N. Shiono, "Interface-Trap Generation at Ultrathin SiO_2 (4 nm-6 nm)-Si Interfaces During Negative-Bias Temperature Aging," *J.Appl.Phys.*, vol. 77, no. 3, pp. 1137–1148, 1995.

[24] A.T. Krishnan, S. Chakravarthi, P. Nicollian, V. Reddy, and S. Krishnan, "Negative Bias Temperature Instability Mechanism: The Role of Molecular Hydrogen," *Appl.Phys.Lett.*, vol. 88, no. 15, pp. 1–3, 2006.

[25] B. Kaczer, V. Arkhipov, R. Degraeve, N. Collaert, G. Groeseneken, and M. Goodwin, "Temperature Dependence of the Negative Bias Temperature Instability in the Framework of Dispersive Transport," *Appl.Phys.Lett.*, vol. 86, no. 14, pp. 1–3, 2005.

[26] D.B. Brown and N.S. Saks, "Time Dependence of Radiation-Induced Trap Formation in Metal-Oxide-Semiconductor Devices as a Function of Oxide Thickness and Applied Field," *J.Appl.Phys.*, vol. 70, no. 7, pp. 3734–3747, 1991.

[27] W.B. Jackson, "Connection between the Meyer-Neldel Relation and Multiple-Trapping Transport," *Phys.Rev.B*, vol. 38, no. 5, pp. 3595–3598, 1988.

QUESTIONS AND ANSWERS

Q1: What is the exact nature of the trap density of states?

A1: This depends on the diffusing species. For H^+, which hops from one bridging oxygen to the next, the binding energies might vary due to the amorphous nature of the material. H_2 would move from one interstitial site to another, where the barriers could vary. Deep traps, like for instance silicon dangling bonds or oxygen vacancies could show up as a Gaussian peak in the density of states.

Q2: Is there a link between the diffusing hydrogen and electrical traps? Could the diffusing hydrogen create traps?

A2: It is certainly possible that diffusing hydrogen creates electrically active traps. For instance, interaction between hydrogen and E' centers have been reported. To take account of that in the model one could differentiate between hydrogen residing in shallow traps, which are the hopping sites and not traps in the strictest sense, and deep traps, which could for instance be identified with E' centers.

Q3: In your figures there is a saturation in the kinetics around 1Ms, what is the E field for the simulation? Did you assume a kf?

A3: The saturation in Figs. 5-7 is due to the hydrogen diffusion front reaching the polysilicon interface where a reflecting boundary condition was assumed. Since the figures show atomic hydrogen results and the electric field enters this model only through the forward rate kf, its exact value does not matter here. For degradations at different electric fields, the assumption that the field-dependence enters only through kf has to be evaluated.